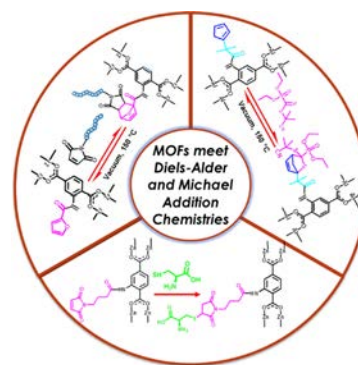


# Reversible Diels–Alder and Michael Addition Reactions Enable the Facile Postsynthetic Modification of Metal–Organic Frameworks

Sana Nayab, Vanessa Trouillet, Hartmut Gliemann, Peter G. Weidler, Iqra Azeem, Saadia R. Tariq, Anja S. Goldmann,\* Christopher Barner-Kowollik,\* and Basit Yameen\*

**ABSTRACT:** Functionalization of metal–organic frameworks (MOFs) is critical in exploring their structural and chemical diversity for numerous potential applications. Herein, we report multiple approaches for the tandem postsynthetic modification (PSM) of various MOFs derived from Zr(IV), Al(III), and Zn(II). Our current work is based on our efforts to develop a wide range of MOF platforms with a dynamic functional nature that can be chemically switched via thermally triggered reversible Diels–Alder (DA) and hetero Diels–Alder (HDA) ligations. Furan tagged MOFs (furan UiO 66 Zr) were conjugated with maleimide groups bearing dienophiles to prepare MOFs with a chemically switchable nature. As HDA pairs, phosphoryl dithioester based moieties and cyclopentadiene (Cp) grafted MOF (Cp MIL 53 Al) were utilized to demonstrate the cleavage and rebonding of the linkages as a function of temperature. In addition to these strategies, the Michael addition reaction was also applied for the tandem PSM of IRMOF 3 Zn. Maleimide groups were postsynthetically introduced in the MOF lattice, which were further ligated with cysteine based biomolecules via the thiol–maleimide Michael addition reaction. On the basis of the versatility of the herein presented chemistry, we expect that these approaches will help in designing a variety of sophisticated functional MOF materials addressing diverse applications.



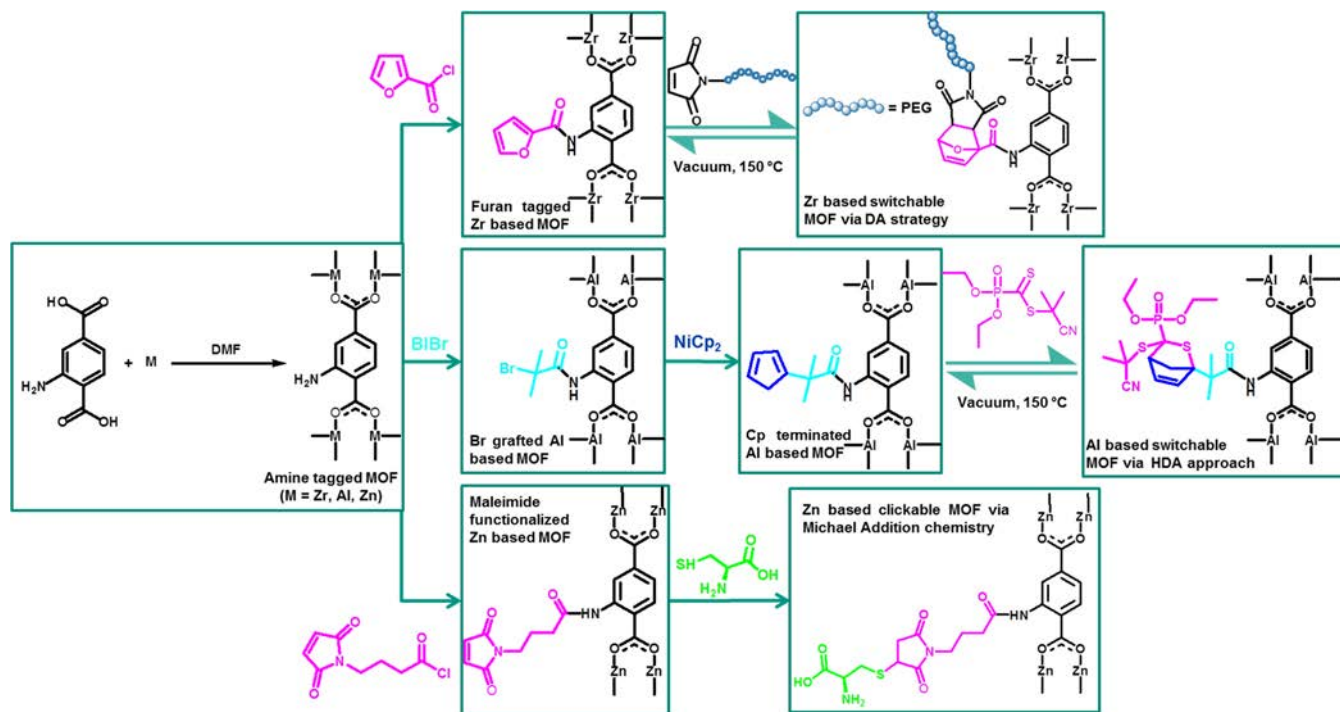
## INTRODUCTION

For a materials chemist, one of the challenges is to develop reliable strategies that help in fine tuning the chemical and physical properties of materials on a molecular level. Metal–organic frameworks (MOFs) are crystalline porous materials composed of metal ions in coordination with organic linkers.<sup>1</sup> Owing to their unique set of properties including large surface area, stability against chemical and thermal treatments, and tunable geometry and pore size, MOFs have gained significant attention and opened new perspectives for diverse applications such as sensing, gas storage, drug delivery, separation, adsorption, and catalysis.<sup>2–5</sup> However, the incorporation of functional moieties into MOF structures, modulating pore chemistry, and hence the optimization of material properties in a controllable manner, remain challenging. Considerable efforts have been invested into designing functional MOF materials through the modification of organic linkers.<sup>6</sup> Postsynthetic modification (PSM) has emerged as a facile tool allowing the fabrication of MOFs with diverse functional moieties, offering a convenient route to chemically tailor the physicochemical properties of MOFs without deforming the lattice structure.<sup>7</sup> The types of chemical linkages that are formed or broken during the postsynthetic reactions divide the PSM approach into three categories including postsynthetic deprotection, dative PSM, and covalent PSM.<sup>8</sup> Rapid progress in the area of the functionalization of MOFs has introduced various new routes beyond PSM. These approaches include postsynthetic

metal exchange or transmetalation where metal ions within the MOFs are replaced in a postsynthetic manner. Alternatively, linkers in MOFs can also be exchanged postsynthetically where the exchange of framework linkers results in the installation of different chemical functionalities in the MOF skeleton. The replacement of linkers can also help in modulating the pore size of MOFs without altering the crystallinity.<sup>9</sup>

For PSM strategies, undoubtedly an amine functionalized linker, 2 amino benzenedicarboxylic acid (NH<sub>2</sub> BDC), has been employed extensively to incorporate amino groups as chemical handles compared to any other functional linker. This preferential choice can be attributed to the relatively simple incorporation of NH<sub>2</sub> BDC into a variety of MOFs and its ability to readily substitute nonfunctionalized 1,4 benzenedicarboxylic acid (BDC) in different prototypical MOF topologies.<sup>8</sup> Among the reported PSM reactions, strategies based on modular ligation chemistry are particularly attractive for efficiently introducing various functional groups with high yield and under mild reaction conditions. To date, within the modular ligation paradigm, several examples of azide–alkyne

**Scheme 1. Schematic Illustration of Tandem Postsynthetic Modification of Zr , Al , and Zn Based MOFs via Reversible Diels–Alder, Hetero Diels–Alder, and Michael Addition Reactions**



cycloaddition reactions<sup>10–15</sup> have been utilized to functionalize MOFs. So far, only a few examples of Diels–Alder (DA) reactions have been reported for the PSM of MOFs. Chen et al. have demonstrated inverse electron demand DA reactions between olefin tagged MOFs and tetrazine.<sup>16</sup> However, Roy et al. have reported DA reactions between MOFs constructed from a furan functionalized linker and maleimides.<sup>17</sup>

Despite exploring the possibility of cycloaddition reactions as a PSM approach for the functionalization of MOFs, the potential for controlled introduction of reversible covalent linkages into various MOF platforms continues to pose a challenge and is yet to be fully explored. The ability of functional materials to reversibly switch their physical and chemical natures in a cyclic fashion under external stimuli including pH, temperature, heat, or light has been extensively studied in material research. In this context, undoubtedly the most broadly explored chemistries include thermoreversible Diels–Alder and hetero Diels–Alder (HDA) reactions. This can be attributed to the availability of various diene and dienophile pairs that allows the tuning of the temperature range for the cleavage and rebonding reactions. Only recently, an NH<sub>2</sub> MIL 88B Fe based reprogrammable MOF platform was developed by our team via DA/retro Diels–Alder (rDA) reactions between a cyclopentadiene (Cp) functionalized MOF and maleimide bearing small units.<sup>18</sup> These MOF systems highlighted the viability of thermally reversible DA reactions as a covalent PSM strategy for the fabrication of chemically switchable MOFs.

While Cp/maleimide based DA reactions offer facile control under which covalent bonds can be broken or formed, furan/maleimide DA reactions have also been employed in a reversible fashion to construct thermally responsive systems.<sup>19</sup> In addition, HDA linkages between the highly reactive cyclopentadiene and phosphoryl dithioester pair exhibit fast bonding debonding behavior within a small temperature

gradient, resulting in a rapid change in the properties of the materials.<sup>20–22</sup>

In addition to cycloaddition reactions, thiol–ene chemistry has been reported in the literature as a PSM method for efficiently introducing functional moieties within the framework of MOFs.<sup>23</sup> In this context, Hindelang et al. reported a thiol–ene reaction between olefin bearing MOFs and ethyl mercaptan.<sup>24</sup> Similarly, Gui et al. have functionalized olefin tagged MOFs with ethanethiol via thiol–ene reactions.<sup>25</sup> Lately, Jiang et al. decorated the methacrylamide functionalized MOFs with thiol side chains bearing polysiloxane oligomers through thiol–ene reactions.<sup>26</sup> However, these reported studies have focused on the radical mediated variant of these reactions and no considerable attention has been paid in the area of PSM involving Michael addition chemistry.<sup>27</sup> Recently, Zhang and Wang et al. controlled the solid state fluorescent photoinduced electron transfer (PET) process in anthracene and maleimide functionalized MOFs via DA as well as thiol–ene reactions.<sup>28</sup>

Herein, we report multiple strategies that—although are conceptually distinct—allow tandem postsynthetic modification of MOFs (Scheme 1). The versatility of these approaches developed herein is demonstrated by encompassing MOFs derived from different metals including Zr, Al, and Zn. First, thermally triggered reversible DA and HDA reactions were employed to fabricate MOFs with conveniently controllable and switchable chemical natures. More precisely, maleimide group containing polymer and small molecule were utilized as dienophiles to perform the DA/rDA reactions with furan functionalized UiO 66 Zr (UiO = University of Oslo) acting as diene. Furthermore, HDA reactions were employed in a reversible manner to modify MIL 53 Al (MIL = Materials from Institute Lavoisier). The HDA diene/dienophile pairs used to demonstrate the chemical bonding debonding reactions were based on cyclopentadiene functionalized MOF and phosphoryl

dithioester moieties. Finally, the Michael addition approach was applied for the postsynthetic modification of IRMOF 3 Zn (isoreticular MOF). Maleimide groups were introduced into the frameworks of IRMOF 3 Zn, which were further utilized to graft a thiol terminated biomolecule, cysteine, through the thiol–maleimide Michael addition reaction at ambient temperature. Due to the large variety of chemically distinct substituents that can be incorporated through the range of ligations employed in the current study, the herein presented work will open avenues to a range of rationally designed chemically diverse MOFs with controllable and switchable chemical nature, making them suitable for application in a wide variety of fields.

## EXPERIMENTAL METHODS

**Materials and Reagents.**  $\alpha$  Bromoisobutyryl bromide (98%), zirconium (IV) chloride ( $ZrCl_4$ , 99.5%), triethylamine (TEA, 99%), zinc nitrate hexahydrate ( $Zn(NO_3)_2 \cdot 6H_2O$ , 98%), *N,N* dimethylformamide (DMF, 99%), dry dichloromethane (DCM, 99.8%), dry tetrahydrofuran (THF, 99.9%), sulfuric acid (95–97%), chloroform ( $CHCl_3$ , 99%), and methanol were obtained from Sigma Aldrich, Germany. 2 Aminoterephthalic acid ( $NH_2$  BDC) (99%) and L cysteine (98%) were received from Alfa Aesar, Germany. Aluminum nitrate nonahydrate ( $Al(NO_3)_3 \cdot 9H_2O$ , 98.5%), 2 furoyl chloride ( $C_3H_3ClO_2$ , 98.0%), and triphenyl phosphine (TPP,  $\geq 99\%$ ) were purchased from Merck, Germany. mPEG Mal (here termed PEG Mal) ( $M_w = 550$ ) was purchased from Creative PEGWorks, Germany. Hydrochloric acid (37%) was purchased from Lab Scan Limited. Bis(cyclopentadienyl)nickel ( $NiCp_2$ , 99%) was received from ABCR GmbH & Co KG, Germany.  $d_6$  DMSO was obtained from Cambridge Isotope Laboratories, Inc. Sodium iodide (NaI) was purchased from Fisher Scientific, U.K. (*N* (3 Bromo propyl) maleimide) (Br Mal),<sup>18</sup> 2 cyanopropan 2 yl(diethoxyphosphoryl)methane dithioate (HDA 1),<sup>29</sup> 4 (((diethoxyphosphoryl)carbonothioyl)thio)methyl benzoic acid (HDA 2),<sup>30</sup> and 4 maleimidobutyryl chloride<sup>31</sup> were synthesized according to literature procedures. Triethylamine (TEA) was dried using calcium hydride and stored under an inert atmosphere.

**Functionalization of  $NH_2$ -UiO-66-Zr MOF via Furan–Maleimide Diels–Alder/Reversible Diels–Alder Reaction as PSM Approach.**  $NH_2$ -UiO-66-Zr Synthesis.  $NH_2$  UiO 66 Zr was prepared following a reported protocol.<sup>32</sup> 2 Aminoterephthalic acid (0.39 g, 2.1 mmol),  $ZrCl_4$  (1 g, 4.2 mmol), and DMF (125 mL) were mixed in a round bottom flask and sonicated to obtain a clear solution. The mixture was kept at 120 °C for 48 h. The resulting powder was isolated by centrifugation, followed by washing with DMF and methanol, and soaked in fresh methanol for 3 days (the solvent was refreshed daily). Finally, the resultant product was obtained by centrifugation, which was then dried at 100 °C under vacuum overnight.

**Synthesis of Furan-Functionalized UiO-66-Zr.** Furan functionalized Zr based MOF was prepared by following the literature procedure.<sup>33</sup>  $NH_2$  UiO 66 Zr (0.2 g), TEA (200  $\mu$ L), and dry THF (8 mL) were introduced into a round bottom flask. Further, 2 furoyl chloride (200  $\mu$ L) was added and the solution was stirred at ambient temperature for 24 h under an inert atmosphere ( $N_2$ ). The resulting product was washed with THF and methanol. Next, the particles were immersed in methanol (24 h) and then separated through centrifugation. The product was dried overnight under vacuum at room temperature.

**Conjugations of Poly(ethylene glycol) Bearing Maleimide to Furan-UiO-66-Zr via DA Ligation.** The DA conjugation between a furan terminated MOF and a maleimide moiety was performed by following the reported protocol.<sup>34</sup> Furan UiO 66 Zr (0.1 g) and PEG Mal (0.048 g) were added to chloroform (3 mL) under an inert atmosphere ( $N_2$ ). The mixture was stirred at room temperature for 24 h. The resulting particles were washed with chloroform and methanol, followed by drying under vacuum at ambient temperature.

**Retro-Diels–Alder Reaction.** The retro Diels–Alder reaction was performed by heating the MOF obtained after the 1st DA reaction at 150 °C under vacuum for 24 h. The product obtained was dried under vacuum at room temperature after washing with  $CHCl_3$ .

**Second Diels–Alder Ligation.** The second Diels–Alder cyclo addition reaction was performed on the product obtained after retro Diels–Alder reaction. MOF (after rDA reaction, procedure can be found above) (0.05 g) and Br Mal (0.025 g) were added to chloroform (1.5 mL) under an inert atmosphere in a flask and stirred at ambient temperature (24 h). The obtained sample was washed with chloroform and methanol followed by drying overnight under vacuum at room temperature.

**Postsynthetic Modification of  $NH_2$ -MIL-53-Al MOFs via Hetero-Diels–Alder/Reversible Hetero-Diels–Alder (HDA) Strategy.** **Synthesis of  $NH_2$ -MIL-53-Al.**  $NH_2$  MIL 53 Al was synthesized by following a reported protocol.<sup>35</sup> 2 aminoterephthalic acid (1.1 g, 6.1 mmol),  $Al(NO_3)_3 \cdot 9H_2O$  (1 g, 2.6 mmol), and DMF (60 mL) were taken in a round bottom flask and sonicated to get a clear solution. The mixture was kept at 130 °C for 48 h. The resulting product was separated by centrifugation, washed with DMF and acetone, and dried at 100 °C under vacuum overnight. Finally, the resulting product was activated in boiling methanol overnight, followed by drying (80 °C) under vacuum.

**Synthesis of Br-Functionalized MIL-53-Al.** Br functionalized MIL 53 Al was prepared according to a reported protocol.<sup>36</sup>  $NH_2$  MIL 53 Al (0.6 g) was taken in dry DCM (12 mL), and then,  $\alpha$  bromoisobutyryl bromide (90  $\mu$ L) and TEA (120  $\mu$ L) were added to this solution under an inert atmosphere ( $N_2$ ), followed by stirring at room temperature (24 h). The obtained product was washed with DCM and methanol and soaked in methanol for 24 h followed by drying under vacuum at ambient temperature.

**Synthesis of Cp-Functionalized MIL-53-Al.** Cp terminated MIL 53 Al was synthesized under an inert atmosphere following a reported protocol.<sup>37</sup> Br MIL 53 Al (0.3 g) was taken in dry THF (12 mL); then NaI (0.041 g), TPP (0.024 g), and  $NiCp_2$  (0.035 g) were added; and the mixture was stirred at room temperature (24 h). The recovered sample was sequentially washed with THF and methanol and soaked in methanol (24 h at room temperature). The sample was subsequently washed with methanol followed by drying under vacuum at ambient temperature.

**Conjugation of Cp-MIL-53-Al with the HDA Moiety via the HDA Reaction.** HDA reactions were employed using literature protocols.<sup>38</sup> Cp MIL 53 Al (0.1 g), HDA 1 (0.03 g), and  $ZnCl_2$  (0.004 g) were added in 3 mL of  $CHCl_3$  and stirred at ambient temperature for 12 h. Subsequently, the sample was washed with  $CHCl_3$  followed by drying under vacuum at ambient temperature.

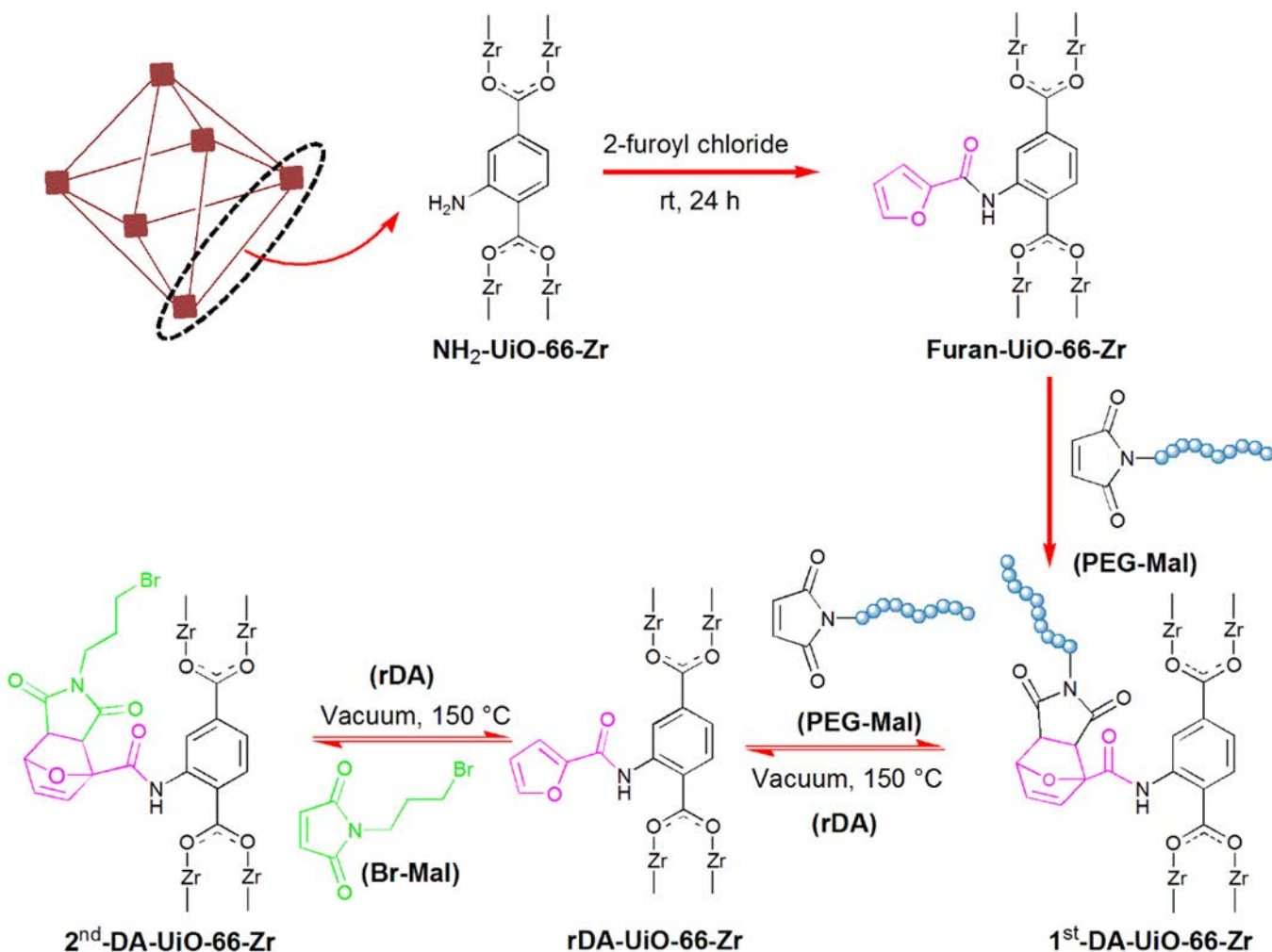
**Retro-HDA Reaction.** The retro Diels–Alder reactions were performed by heating the MOF obtained after 1st HDA conjugation at 150 °C under vacuum (24 h) followed by washing with  $CHCl_3$  and drying the product under vacuum at ambient temperature.

**Second Hetero-Diels–Alder Ligation.** The second hetero Diels–Alder ligation was performed to support our idea that the MOFs after rDA could be reused. MOF (obtained after rDA; procedure can be found above) (0.1 g), HDA 2 (0.03 g), and  $ZnCl_2$  (0.004 g) were added in 3 mL of  $CHCl_3$  and stirred at ambient temperature (12 h). Subsequently, the product was washed with  $CHCl_3$  followed by drying under vacuum at ambient temperature.

**Postsynthetic Modification of IRMOF-3-Zn via the Michael Addition Click Reaction.** **Synthesis of IRMOF-3-Zn.** IRMOF 3 Zn was synthesized according to the method adapted from the literature.<sup>39</sup> 2 aminoterephthalic acid (0.3 g, 1.6 mmol),  $Zn(NO_3)_2 \cdot 4H_2O$  (1.2 g, 4.5 mmol), and DMF (30 mL) were mixed in a flask and dissolved under sonication to get a clear solution, which was heated at 105 °C (48 h). The product obtained after centrifugation was thoroughly washed with dry DMF and  $CHCl_3$  and then suspended in dry  $CHCl_3$  for 3 days (solvent was refreshed daily). Afterward, the solvent was decanted followed by drying the obtained crystals (80 °C under vacuum for 24 h).

**Synthesis of Maleimide-Functionalized IRMOF-3-Zn.** Maleimide functionalized IRMOF 3 Zn was prepared by following the literature

Scheme 2. Preparation of Zirconium Based Switchable MOFs through a Furan–Maleimide DA/rDA Approach



protocol.<sup>40</sup> IRMOF 3 Zn (0.1 g), TEA (50  $\mu$ L), and 4 maleimido butyryl chloride (0.053 g) were stirred (24 h) in dry THF (3 mL) under an inert atmosphere (N<sub>2</sub>). The resulting product was subjected to sequential washing with THF and then with methanol that removed the quaternary ammonium salt that was formed during the reaction. Afterward, the particles were dried under vacuum at room temperature.

*Modification of Mal-IRMOF-3-Zn via the Thiol–Maleimide Michael Addition Reaction.* Mal IRMOF 3 Zn (0.05 g), cysteine (0.028 g), and methanol (3 mL) were taken in a round bottom flask. To this solution, TEA (0.04 mL) was added and allowed to stir at ambient temperature (24 h). The product was subjected to washing with methanol and drying under vacuum overnight.

## RESULTS AND DISCUSSION

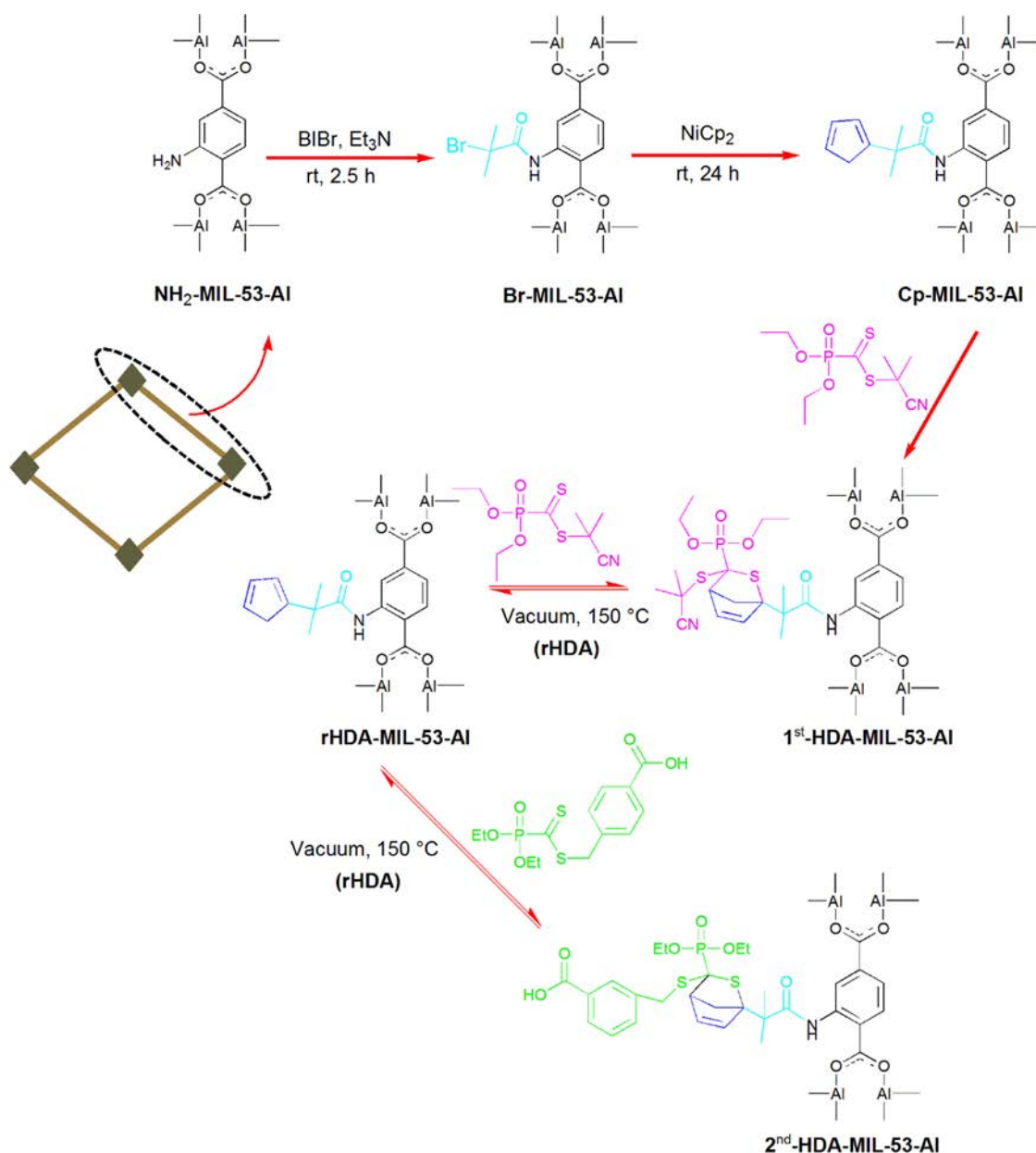
A furan–maleimide based DA approach was employed to fabricate Zr derived MOF with a switchable chemical nature (Scheme 2). NH<sub>2</sub> UiO 66 Zr was prepared by employing a 2 aminobenzenedicarboxylic acid (NH<sub>2</sub> BDC) linker. Furan groups were incorporated into the framework by reacting the amino moieties present in the synthesized MOF with 2 furoyl chloride. The DA conjugation reaction between furan functionalized MOF (furan UiO 66 Zr) and maleimide groups, PEG Mal and Br Mal, was executed at room temperature in chloroform. The DA conjugation was followed by a reversible DA ligation at 150 °C under vacuum.

Furthermore, Al based MOF was modified through HDA conjugations with the aim of introducing reversibly cleavable linkages (Scheme 3). NH<sub>2</sub> MIL 53 Al was prepared using an NH<sub>2</sub> BDC linker. The amino groups present within the frameworks were subsequently treated with  $\alpha$  bromoisobutyryl bromide to prepare bromo tagged MOF. Further, nickelocene (NiCp<sub>2</sub>) was employed to transform bromo groups into Cp moieties. The coupling reaction between Cp functionalized MOF (Cp MIL 53 Al) and phosphoryl dithioesters (HDA 1 and HDA 2) was performed in chloroform at ambient temperature in the presence of zinc chloride. The HDA cycloreversion reaction between Cp MIL 53 Al and HDA 1/HDA 2 was performed at 150 °C under vacuum.

Moreover, Michael addition was employed to demonstrate the postsynthetic modification of IRMOF 3 Zn MOF (Scheme 4). The IRMOF 3 Zn was synthesized using NH<sub>2</sub> BDC as the linker. The amino moieties within the structure of IRMOF 3 Zn were treated with 4 maleimidobutyryl chloride to obtain the maleimide tagged MOFs. Further, the thiol–maleimide Michael addition approach employed exploiting the reactivity of maleimide bearing frameworks toward thiols for the grafting of cysteine in the presence of TEA as a catalyst at ambient conditions.

Scanning electron microscopy (SEM) revealed the morphology of the synthesized and modified MOFs (Figure 1). Intergrown small crystals with grain sizes close to 100 nm were

Scheme 3. Synthetic Approach for the Preparation of Aluminum Derived Switchable MOFs via Reversible HDA Linkages



observed for NH<sub>2</sub> UiO 66 Zr. The crystals of NH<sub>2</sub> MIL 53 Al were rod shaped with a length close to 200 nm and a diameter close to 60 nm. In the case of IRMOF 3 Zn, the SEM images revealed a wide diversity in size ranging from submicron sized crystals to the crystal up to 80 μm in size. The crystal morphologies of all MOF systems were well retained throughout the modification of MOFs, and no crystal collapse was observed.

The X ray powder diffraction (XRD) studies exhibited that the MOF materials were crystalline and the observed XRD peaks were in accordance with the literature patterns of NH<sub>2</sub> UiO 66 Zr,<sup>41</sup> NH<sub>2</sub> MIL 53 Al,<sup>42</sup> and IRMOF 3 Zn<sup>43</sup> (Figure 2). Furthermore, the frameworks remained crystalline after the modification steps via the ligation reactions. The cell parameter data is provided in Tables S1–S3. The peaks obtained in the XRD diffractogram of NH<sub>2</sub> UiO 66 were indexed in the cubic space group *Fm3m*, and the unit cell volume was determined to be 8834.2 Å<sup>3</sup>, which further increased to 8914.0 Å<sup>3</sup> after the

functionalization with furan groups and changed to 8877.4 and 8949.1 Å<sup>3</sup> after the 1st and 2nd DA reactions, respectively. These values reflect on the incorporation of the guest moieties in the pore channels of the framework.<sup>44</sup> The XRD pattern of NH<sub>2</sub> MIL 53 Al showed the monoclinic *Cc* phase, and the values of cell volume suggest the breathing nature of NH<sub>2</sub> MIL 53 Al upon grafting of different molecules.<sup>45</sup> The cell volume of NH<sub>2</sub> MIL 53 Al decreased from 979.3 to 895.3 and 974.4 Å<sup>3</sup> after the first and second HDA based click reactions, respectively. The integration of bulky functional groups caused a decrease in cell volume due to the excess loading and the associated filling of the pores.<sup>46</sup> The shifts of the position and differences in the intensity of the reflections are attributed to the structural flexibility and movement of the framework upon incorporation of the guest moieties in the pores of the MOFs. The XRD diffractogram of IRMOF 3 Zn suggested a trigonal symmetry with the *R3m* space group. The cell volume of the IRMOF 3 Zn framework decreased after employing Michael

Scheme 4. Postsynthetic Modification of Zinc Based MOFs via the Michael Addition Reaction

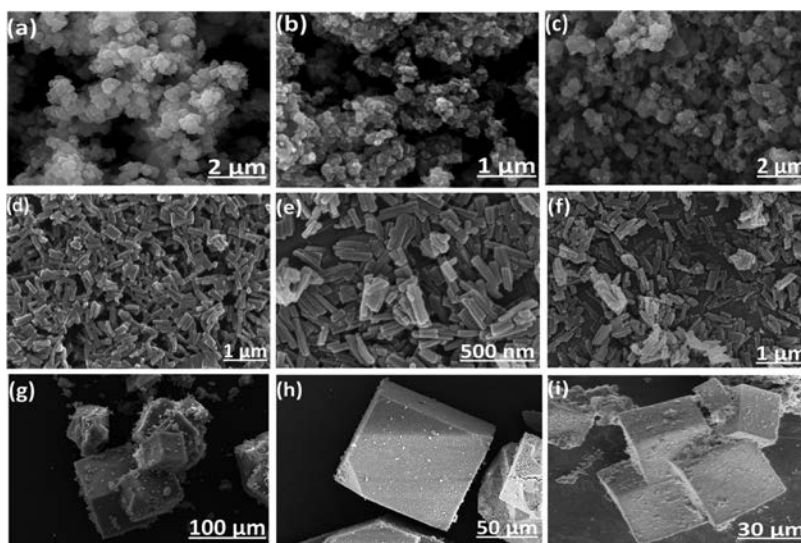
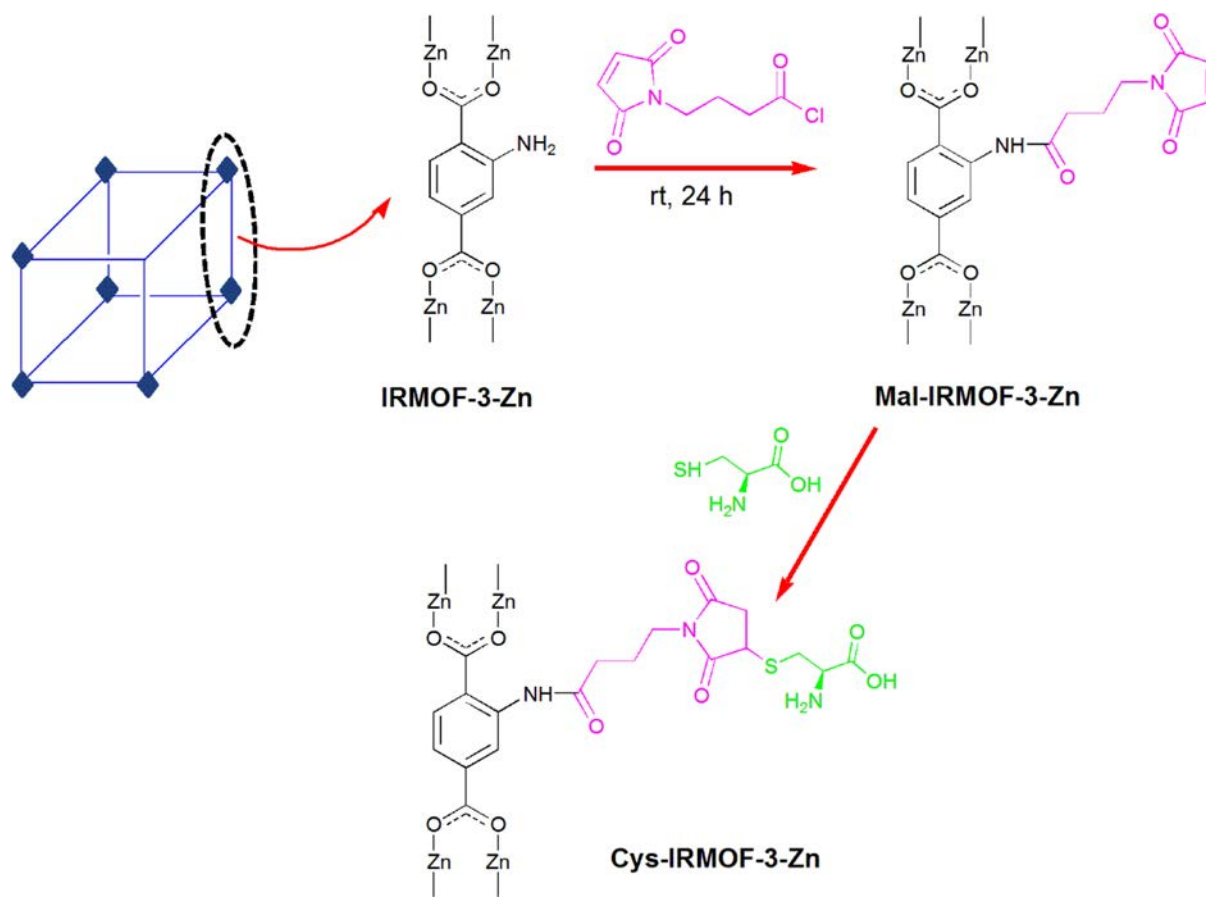
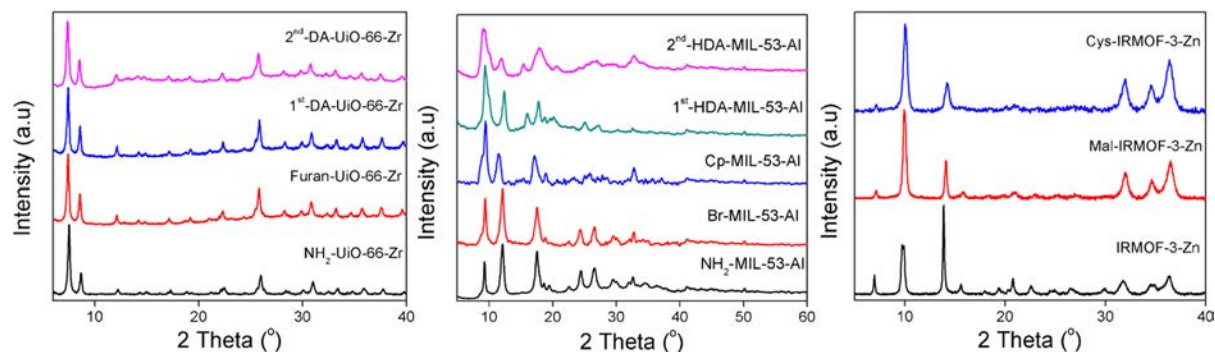


Figure 1. SEM images of (a) NH<sub>2</sub> UiO 66 Zr, (b) 1st DA UiO 66 Zr, (c) 2nd DA UiO 66 Zr, (d) NH<sub>2</sub> MIL 53 Al, (e) 1st HDA MIL 53 Al, (f) 2nd HDA MIL 53 Al, (g) IRMOF 3 Zn, (h) Mal IRMOF 3 Zn, and (i) Cys IRMOF 3 Zn.

addition from 12744.8 to 12319.2 Å<sup>3</sup>. The XRD pattern did not exhibit substantial shifts in the position of the peaks; however, a tendency toward reduced peak intensity was observed. Such differences in the intensity of XRD reflections of MOFs are common and may be assigned to the pore filling by the guest species. In the case of MOF materials, where large voids are available to the guest molecules, the intensity of XRD peaks (mainly at low  $2\theta$  angles) strongly depends upon the

extent of pore filling and the scattering power of the guest moieties. For IRMOF 3 Zn, the second reflection at  $9.7^\circ$  was visibly strongest after the modifications and was in agreement with the literature. The higher extent of pore filling led to the observed increase in the reflection intensity at  $9.7^\circ$ .<sup>47</sup>

All chemical modifications were substantiated via X ray photoelectron spectroscopy (XPS). In the case of NH<sub>2</sub> UiO 66 Zr, the presence of amino groups was verified by the



**Figure 2.** XRD patterns of  $\text{NH}_2$  UiO 66 Zr (left),  $\text{NH}_2$  MIL 53 Al (middle), and IRMOF 3 Zn (right) before and after the modifications.

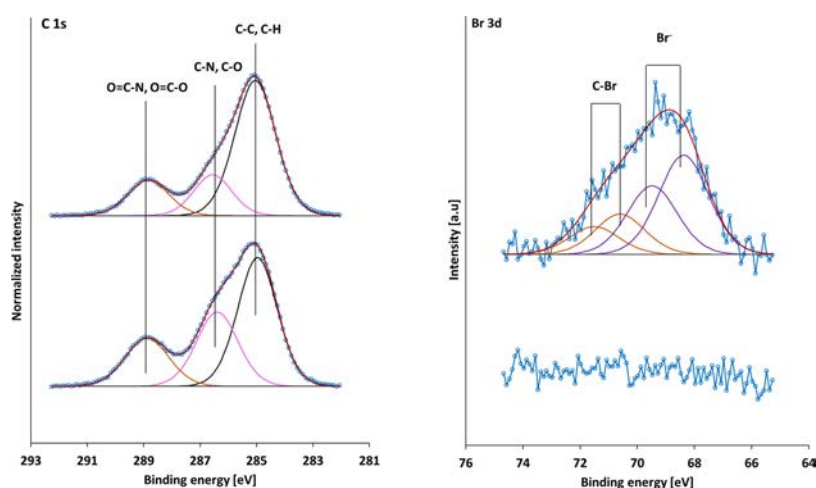


**Figure 3.** C 1s and Br 3d high resolution XPS spectra corresponding to the  $\text{NH}_2$  UiO 66 Zr series during different modification stages. Left side (C 1s): 1st DA UiO 66 Zr (bottom), rDA UiO 66 Zr (top). Right side (Br 3d): rDA UiO 66 Zr (bottom) and 2nd DA UiO 66 Zr (top). For the purpose of better visualization, all of the C 1s spectra have been normalized to the maximum of the intensity.

presence of the N 1s signal at 399.7 eV,<sup>48</sup> which is associated with amino groups. This signal was accompanied by a second peak at 401.3 eV that can be attributed to the protonated amino groups. All subsequent samples resulting from the reactions depicted in Scheme 2 showed a clear N 1s signal at a shifted binding energy of 400.1 eV, which supports the introduction of amide and maleimide groups. The further reaction steps, specifically the functionalization with furan and the conjugation of PEG Mal and Br Mal to the furan functionalized frameworks via 1st DA and 2nd DA reactions, respectively, were followed by the C 1s XPS spectra (Figure 3) through considering the ratio of (C–O, C–N)/(C–C, C–H) (refer to Figure 4). The increase in the intensity of the peak at 286.4 eV (C–O, C–N) for furan UiO 66 Zr clearly showed the success of furan functionalization. A further increase in the ratio of (C–O, C–N)/(C–C, C–H) confirmed the successful grafting of polyethylene glycol after the 1st DA step. This ratio was subsequently found to decrease from  $\sim 0.6$  to  $\sim 0.3$  after cyclereversion for rDA UiO 66 Zr, indicating the thermally triggered rDA reaction between maleimide moieties and furan functionalized MOFs. The presence of the Br 3d doublet with Br 3d<sub>5/2</sub> at 70.5 eV confirmed the conjugation of furan functionalized UiO 66 Zr with Mal Br during the 2nd DA reactions (Figure 3). The doublet for Br 3d<sub>5/2</sub> at 68.0 eV suggests the capturing of noncovalently attached bromine ( $\text{Br}^-$ ) into the framework. However, the presence of  $\text{Br}^-$  did not affect the DA ligations.<sup>18</sup>

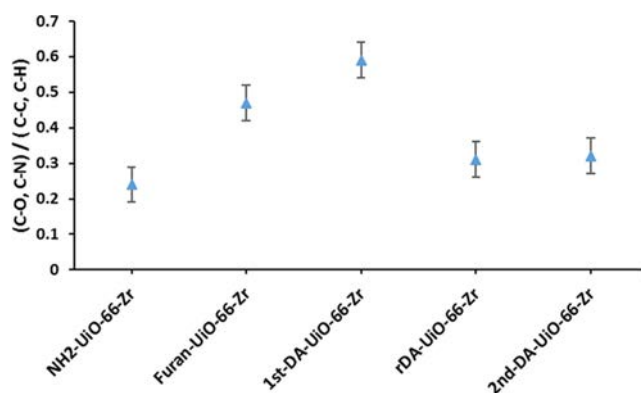


**Figure 4.** (C–N, C–O)/(C–C, C–H) ratio calculated from the XPS quantitative analysis of Zr based MOFs after employing 1st and 2nd Diels–Alder reactions. (C–N, C–O)/(C–C, C–H) ratio obtained from XPS analysis of  $\text{NH}_2$  UiO 66 Zr and furan UiO 66 Zr are also provided for comparison. The C 1s signal fitted by three peaks (285.0, 286.6, and 288.8 eV) represents (C–C, C–H), (C–N, C–O), and (O–C=O, N–C=O) components.

Similarly, the signal at 399.7 eV<sup>48</sup> corresponding to the N 1s orbital corroborates the presence of amino groups within the framework of  $\text{NH}_2$  MIL 53 Al (Table S4). Furthermore, the subsequent grafting of bromo moieties into the MOF structure was ascertained by the appearance of a peak at 70.1 eV<sup>38</sup> (Br 3d<sub>5/2</sub>), attributed to the bromine covalently attached to carbon

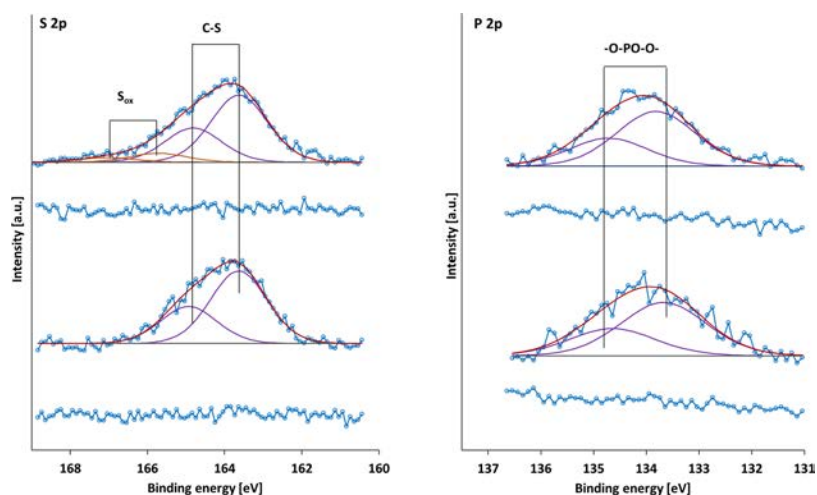


**Figure 5.** S 2p (left) and P 2p (right) high resolution XPS scans of NH<sub>2</sub> MIL 53 Al series during different modification stages: Cp MIL 53 Al, 1st HDA MIL 53 Al, rHDA MIL 53 Al, and 2nd HDA MIL 53 Al are aligned moving from bottom toward top of the figure.

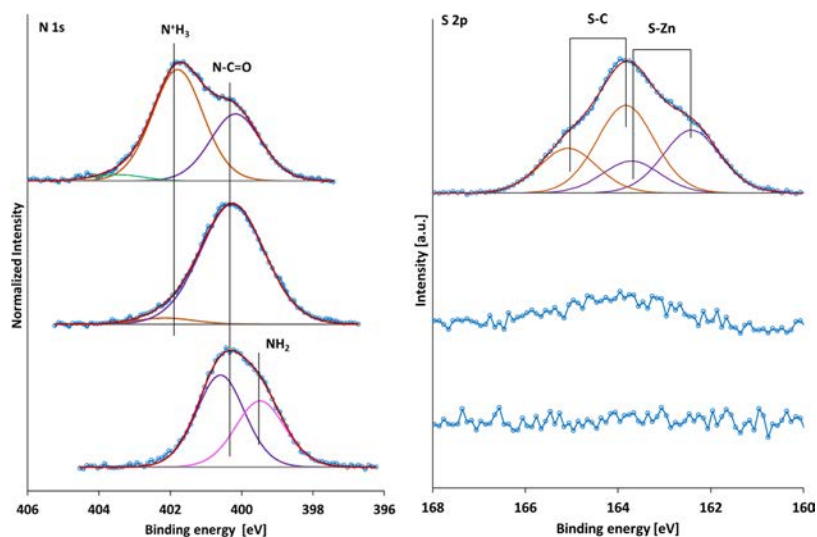


**Figure 6.** N 1s (left) and S 2p (right) XPS spectra of IRMOF 3 Zn series during different modification stages. From bottom to top: IRMOF 3 Zn, Mal IRMOF 3 Zn, and Cys IRMOF 3 Zn. For the purpose of better visualization, all of the N 1s spectra have been normalized to the maximum of intensity.

and the observed N 1s signal at 399.9 eV, indicating the presence of amide groups in Br MIL 53 Al. The partial replacement of the bromo groups by the cyclopentadiene (Cp) moiety resulted in a decrease of the bromine concentration (covalently bound) from 1.7 atomic percent (atom %) down to 1.0 atom %, suggesting a conversion degree of around 40% for the transformation of bromo groups of Br MIL 53 Al to the Cp groups, resulting in the formation of Cp MIL 53 Al. The further successful conjugation of the Cp functionalized framework (Cp MIL 53 Al) with HDA 1 (dienophile) was evidenced by the appearance of a S 2p doublet with S 2p<sub>3/2</sub> at 163.7 eV<sup>49</sup> and a P 2p doublet with P 2p<sub>3/2</sub> at 133.8 eV<sup>50</sup> (Figure 5) in the spectra of 1st HDA MIL 53 Al. Cycloreversion was executed at 150 °C for 24 h, which resulted in the recovery of Cp tagged MOFs ready for another HDA reaction. The reversible HDA reaction between dithioester based HDA moieties and Cp groups was observed for rHDA MIL 53 Al, as verified by the disappearance of the P 2p<sub>3/2</sub> and S 2p<sub>3/2</sub> signals at 133.8 and 163.7 eV, respectively. The second HDA cycloaddition reaction was performed

between the MOFs (postcycloreversion) and HDA 2 (dienophile). The reappearance of the signals at 163.7 eV for S 2p<sub>3/2</sub> and at 133.8 eV for P 2p<sub>3/2</sub> supported the idea of reversibility and switching of chemical functionalities.

Finally, the different reaction steps of PSM of IRMOF 3 Zn were investigated through XPS analysis. The appearance of a N 1s peak at 399.4 eV<sup>48</sup> confirmed the presence of amino groups in IRMOF 3 Zn (Table S5), accompanied by another peak at 400.5 eV, which could eventually stem from an unexpected amide group at this step. The successful grafting of maleimide groups on IRMOF 3 Zn is supported by the slight shift toward the smaller binding energy of the C 1s component from 289.0 to 288.7 eV,<sup>40</sup> suggesting the presence of both O=C=O and N=C=O groups (Figure S1). At the same time, the typical peak associated with the amine disappeared and only amide and maleimide were clearly detected with the N 1s signal at 400.2 eV accompanied by a further peak at 401.8 eV, indicating some protonated nitrogen (Figure 6). The subsequent Michael addition between maleimide functionalized MOF (Mal IRMOF 3 Zn) and cysteine<sup>49</sup> was evidenced



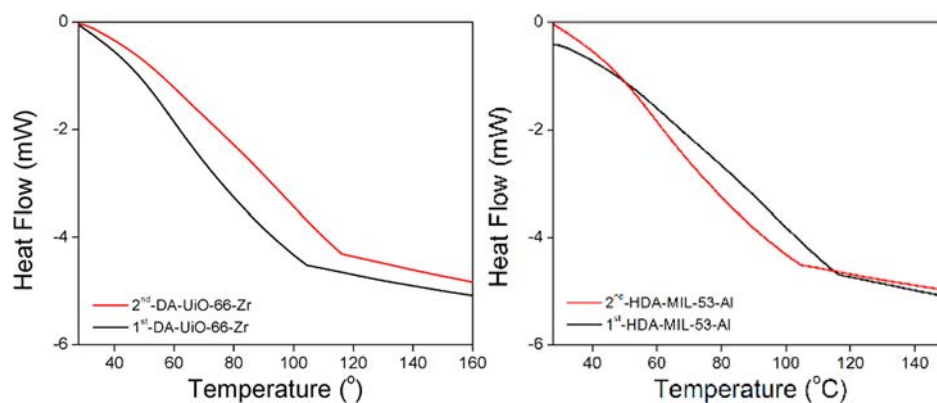


**Figure 7.** DSC thermograms of NH<sub>2</sub> UiO 66 Zr (left) and NH<sub>2</sub> MIL 53 Al (right) indicating the endothermic transitions between 104 and 116 °C corresponding to rDA and rHDA reactions following the 1st and 2nd DA and HDA ligations.

by the clear presence of a S 2p doublet with S 2p<sub>3/2</sub> at 163.8 eV<sup>51</sup> corresponding to covalently bound sulfur in Cys IRMOF 3 Zn (Figure 6). In addition, the N 1s signals appeared at 401.8 eV, suggesting the presence of protonated amine groups in Cys IRMOF 3 Zn. The nitrogen concentration (4.5 atom %), which was close to the concentration of covalently bound sulfur (4.2 atom %), also confirmed the successful grafting of cysteine molecules. The second doublet with S 2p<sub>3/2</sub> at 162.3 eV might be ascribed to the formation of Zn S due to the presence of some Zn in the framework.<sup>52</sup> Hence, the XPS analysis confirmed the successful postsynthetic modification of MOFs by employing various ligation chemistry strategies. It is worth mentioning here that the percentage conversions estimated for various chemical transformations using the XPS data correspond to only the surface moieties confined within the limited sampling depth of the XPS analysis (5–10 nm).<sup>18,36,53,54</sup> For estimating the overall percentage of the chemical transformations across the entire sample, we performed <sup>1</sup>H NMR analysis on the samples obtained after different PSMs reported in this work. The <sup>1</sup>H NMR data is especially important considering large size and associated hindered diffusion through the MOF lattice of some of the molecules that are employed in the PSMs reported in this work.

While XPS analysis ascertained all of the PSMs by revealing the surface chemical compositions of the modified MOF samples, we also employed <sup>1</sup>H NMR spectroscopy (Figures S2–S5) to estimate the overall percentage conversion of the functional groups in the entire MOF sample as a result of the PSMs applied in this study. All MOFs were digested in aqueous acidic medium to disassemble the metal–organic framework before performing the NMR analysis. The <sup>1</sup>H NMR spectra of the digested parent MOFs (NH<sub>2</sub> UiO 66 Zr, NH<sub>2</sub> MIL 53 Al, and IRMOF 3 Zn) clearly exhibited three resonance signals associated with the three aromatic protons of the NH<sub>2</sub> BDC organic linker (Figure S2). The percentage conversions for PSMs were calculated by comparing the resonance integral for the aromatic proton available at the ortho position (marked as “b” in Figure S2) on the benzene ring with respect to the amine/amide substituents on the unmodified and modified dicarboxylate organic linker (NH<sub>2</sub> BDC). This proton is designated as the reference proton in the rest of the discussion. The percentage conversion for the reaction of the amino group of NH<sub>2</sub> UiO 66 Zr with 2 furoyl chloride could be estimated by comparing the resonance integral for the reference proton with the resonance integral for

any of the protons available at position 2, 3, or 4 of the furoyl substituent. The protons at positions 2 (marked as “b” in Figure S3, bottom) and 3 (marked as “a” in Figure S3, bottom) of the furoyl ring appearing at 6.7 and 7.3 ppm were clear from the cluster of signals for the aromatic protons of the linker and were used to estimate the percentage conversions. The percentage conversion for the transformation of NH<sub>2</sub> UiO 66 Zr to furan UiO 66 Zr was estimated to be around 26%. The quantification of the percentage conversions for the first and second DA reactions on furan UiO 66 Zr using NMR spectroscopy could not be performed because the digestion of 1st DA UiO 66 Zr and 2nd DA UiO 66 Zr did not result in clear solutions. The percentage conversion for the transformation of NH<sub>2</sub> MIL 53 Al to Br MIL 53 Al was estimated by comparing the resonance integral for the reference proton with the resonance integral for the methyl groups of the  $\alpha$  isobutyryl substituent. The methyl groups of the  $\alpha$  isobutyryl substituent appeared at 1.85 ppm (marked as “a” in Figure S4, bottom left), and the percentage conversion for the transformation of NH<sub>2</sub> MIL 53 Al to Br MIL 53 Al was estimated to be around 35%. The overall percentage conversion for the transformation of bromo groups of Br MIL 53 Al to Cp groups and the subsequent HDA reactions was estimated by comparing the resonance integral for the reference proton with the resonance integral for the alkene protons of the products of first (1st HDA MIL 53 Al) and second (2nd HDA MIL 53 Al) HDA reactions. The resonance signals for the alkene protons of the products of first and second HDA reactions appeared at around 6.26 and 6.24 ppm (marked as “a” in Figure S4, bottom right), respectively. The percentage conversions estimated by comparing the resonance integrals for the reference proton and alkene protons of the HDA reactions was around 22% for 1st HDA MIL 53 Al and 18% for 2nd HDA MIL 53 Al. The demonstration of Michael addition reaction as a viable PSM strategy involved the reaction of amino groups of IRMOF Zn with 4 maleimidobutyryl chloride. This resulted in the synthesis of Mal IRMOF Zn, offering maleimide groups for the subsequent Michael addition reaction. The presence of maleimide functional groups in Mal IRMOF Zn was confirmed by the appearance of proton resonance characteristic of the maleimide group at around 6.96 ppm (marked as “a” in Figure S5, bottom). The proton resonance for the maleimide group was observed to disappear in the <sup>1</sup>H NMR spectrum of Cys IRMOF Zn that was produced as result of the Michael addition reaction between the maleimide groups of Mal IRMOF Zn and thiol

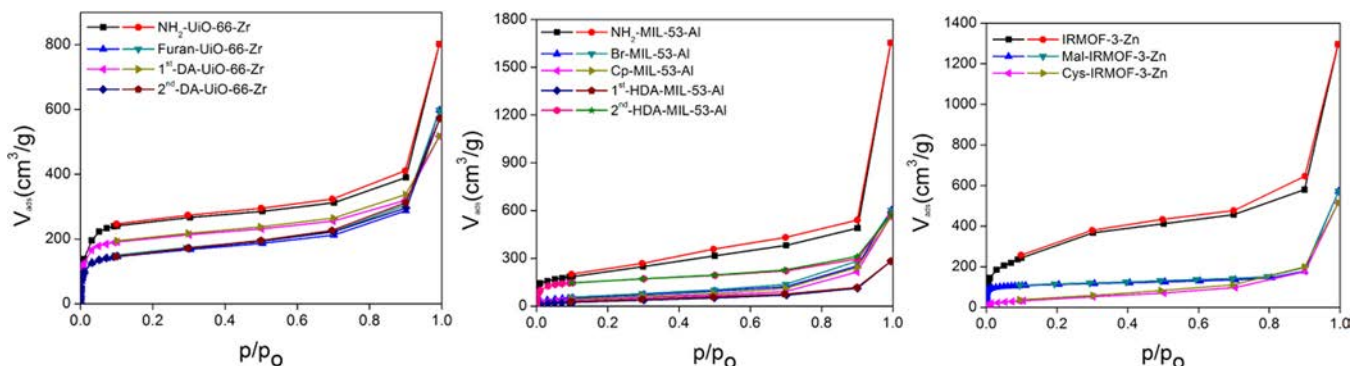


**Figure 8.** Ar adsorption/desorption isotherms for  $\text{NH}_2$  UiO 66 Zr (left),  $\text{NH}_2$  MIL 53 Al (middle), and IRMOF 3 Zn (right) before and after the modifications.

group of cysteine. This observation suggests a quantitative transformation of Mal IRMOF Zn to Cys IRMOF Zn. The quantification of the percentage conversion during the Michael addition reaction by comparing the proton resonance integrals could not be performed because of the close association of the maleimide proton resonance with a broad resonance signal for protons of water. The less than quantitative conversions for all of the PSMs applied in this study, as revealed by the  $^1\text{H}$  NMR spectroscopic analysis, can be attributed to the difficulty faced by the reactants in diffusing through the pores of the MOFs and reaching to all of the linker groups of the solid MOF samples. Complementing the XPS analysis, the overall percentage conversions estimated by the  $^1\text{H}$  NMR spectroscopic analysis provide insight into the depth of the PSMs applied in this study.

Differential scanning calorimetry (DSC) measurements demonstrated the temperature ranges for the retro DA reactions (Figure 7). For Zr and Al based MOFs, the endothermic transitions were witnessed in the temperature range of 104–116 °C. The endothermic transitions corroborate the rDA reactions and retrieval of the initial reactivity of furan and Cp functionalized MOFs for subsequent DA and HDA reactions. These results demonstrate the applicability of the cycloreversion reactions to fabricate a wide range of MOF systems, capable of tuning their functional nature by switching their chemical functionality.

The Ar adsorption/desorption isotherms of nonfunctionalized and functionalized MOFs were obtained at 87 K (Figure 8). The BET surface area of the  $\text{NH}_2$  UiO 66 Zr MOF decreased from 886 to 682 and 523  $\text{m}^2/\text{g}$  upon functionalization via 1st and 2nd DA, respectively, whereas the BET surface area of synthesized  $\text{NH}_2$  MIL 53 Al decreased from 670 to 105  $\text{m}^2/\text{g}$  after employing the 1st HDA reaction and to 153  $\text{m}^2/\text{g}$  after employing the 2nd HDA reaction. The IRMOF 3 Zn exhibited a surface area of 826  $\text{m}^2/\text{g}$ , which subsequently decreased to 151  $\text{m}^2/\text{g}$  after the grafting of cysteine molecule through the Michael addition reaction. The BET surface areas of the as synthesized herein reported MOFs are comparable to the values reported in the literature for the similar MOF systems:  $\text{NH}_2$  UiO 66 Zr (801  $\text{m}^2/\text{g}$ ),<sup>55</sup>  $\text{NH}_2$  MIL 53 Al (427  $\text{m}^2/\text{g}$ ),<sup>56</sup> and IRMOF 3 Zn (812  $\text{m}^2/\text{g}$ ).<sup>56</sup> The details of surface area and total pore volume are provided in Table S6. The plots for pore size distribution and cumulative pore volume are given in Figures S6–S8. A large decrease in surface area and pore volume of MOFs after all of the functionalization steps confirmed that the installation of chemical moieties was mostly inside of the channel of the MOF structures.

## CONCLUSIONS

We have successfully highlighted the significance of various ligation strategies as tandem PSM tools for the fabrication of Zr, Al, and Zn based MOFs. Reversible DA and HDA ligations were applied to  $\text{NH}_2$  UiO 66 Zr and  $\text{NH}_2$  MIL 53 Al MOFs, demonstrating the switching of chemical functionalities within MOF lattices. The reversible DA ligation on the  $\text{NH}_2$  UiO 66 Zr MOF was established through a furan/maleimide coupling pair, while reversible HDA conjugation was established by employing a reversible reaction between Cp and dithioester groups. In addition, the thiol–maleimide Michael addition was demonstrated as a postsynthetic modification strategy for IRMOF 3 Zn. Overall, the herein reported strategies offer avenues for the preparation of MOFs with controlled as well as switchable chemical nature. We submit that these approaches can be extended to other MOF materials and pave a way for fabrication of functional MOFs for a variety of applications.

## AUTHOR INFORMATION

### Corresponding Authors

**Anja S. Goldmann** – *Macromolecular Architectures, Institut für Technische Chemie und Polymerchemie, Karlsruhe Institute of Technology (KIT), 76131 Karlsruhe, Germany; Centre for Materials Science, School of Chemistry and Physics, Queensland University of Technology (QUT), Brisbane, QLD 4000, Australia;* [orcid.org/0000-0002-1597-2836](https://orcid.org/0000-0002-1597-2836); Email: [a.goldmann@qut.edu.au](mailto:a.goldmann@qut.edu.au)

**Christopher Barner Kowollik** – *Macromolecular Architectures, Institut für Technische Chemie und Polymerchemie, Karlsruhe Institute of Technology (KIT), 76131 Karlsruhe, Germany; Centre for Materials Science, School of Chemistry and Physics, Queensland University of Technology (QUT), Brisbane, QLD 4000, Australia;* [orcid.org/0000-0002-6745-0570](https://orcid.org/0000-0002-6745-0570);

Email: christopher.barner.kowollik@kit.edu,  
christopher.barnerkowollik@qut.edu.au

**Basit Yameen** – Department of Chemistry & Chemical Engineering, Syed Babar Ali School of Science and Engineering, Lahore University of Management Sciences (LUMS), Lahore, Punjab 54792, Pakistan; [orcid.org/0000 0002 4359 8394](https://orcid.org/0000-0002-4359-8394); Email: basit.yameen@lums.edu.pk

## Authors

**Sana Nayab** – Department of Chemistry & Chemical Engineering, Syed Babar Ali School of Science and Engineering, Lahore University of Management Sciences (LUMS), Lahore, Punjab 54792, Pakistan; Department of Chemistry, Lahore College for Women University, Lahore, Punjab 54000, Pakistan

**Vanessa Trouillet** – Institute for Applied Materials (IAM), and Karlsruhe Nano Micro Facility (KNMF), Karlsruhe Institute of Technology (KIT), 76344 Eggenstein Leopoldshafen, Germany

**Hartmut Gliemann** – Institute of Functional Interfaces (IFG), Karlsruhe Institute of Technology (KIT), 76344 Eggenstein Leopoldshafen, Germany

**Peter G. Weidler** – Institute of Functional Interfaces (IFG), Karlsruhe Institute of Technology (KIT), 76344 Eggenstein Leopoldshafen, Germany

**Iqra Azeem** – Department of Chemistry & Chemical Engineering, Syed Babar Ali School of Science and Engineering, Lahore University of Management Sciences (LUMS), Lahore, Punjab 54792, Pakistan

**Saadia R. Tariq** – Department of Chemistry, Lahore College for Women University, Lahore, Punjab 54000, Pakistan

## Author Contributions

The manuscript was written through contributions of all authors. All authors have given approval to the final version of the manuscript.

## Notes

The authors declare no competing financial interest.

## ACKNOWLEDGMENTS

B.Y. acknowledges the support from HFSP (RGY0074/2016), HEC for NRPU (Project No. 20 1740/R&D/10/3368, 20 1799/R&D/10 5302, and 5922), TDF 033 grants, and LUMS for start up fund and FIF grant. C.B. K. acknowledges the Australian Research Council (ARC) for funding in the context of a Laureate Fellowship as well as continued support by the Queensland University of Technology (QUT). S.N. acknowledges the funding from the Higher Education Commission (HEC) of Pakistan under the Indigenous Ph.D. 5000 Fellowship Program and IRSIP. The authors appreciate the assistance of Murtaza Saleem from LUMS, Mohamed Tawheed Abdel Razek from KIT, and Sonia Zulfiqar from NUST in SEM and TGA/DSC analyses. Additionally, Ishtiaq Ahmed, Silvana Hurtle, Marcel Langer, and Alexander M. Schenzel from KIT are acknowledged for their assistance in the synthesis of 4 maleimidobutyroyl chloride, Br Mal, HDA 1, and HDA 2.

## REFERENCES

- (1) Stock, N.; Biswas, S. Synthesis of Metal Organic Frameworks (MOFs): Routes to Various MOF Topologies, Morphologies, and Composites. *Chem. Rev.* **2012**, *112*, 933–969.
- (2) James, S. L. Metal organic frameworks. *Chem. Soc. Rev.* **2003**, *32*, 276–288.
- (3) Safaei, M.; Foroughi, M. M.; Ebrahimpoor, N.; Jahani, S.; Omid, A.; Khatami, M. A review on metal organic frameworks: Synthesis and applications. *TrAC, Trends Anal. Chem.* **2019**, *118*, 401–425.
- (4) Jiao, L.; Seow, J. Y. R.; Skinner, W. S.; Wang, Z. U.; Jiang, H. L. Metal–organic frameworks: Structures and functional applications. *Mater. Today* **2019**, *27*, 43–68.
- (5) Yuan, S.; Feng, L.; Wang, K.; Pang, J.; Bosch, M.; Lollar, C.; Sun, Y.; Qin, J.; Yang, X.; Zhang, P.; Wang, Q.; Zou, L.; Zhang, Y.; Zhang, L.; Fang, Y.; Li, J.; Zhou, H. C. Stable Metal–Organic Frameworks: Design, Synthesis, and Applications. *Adv. Mater.* **2018**, *30*, No. 1704303.
- (6) Ali Akbar Razavi, S.; Morsali, A. Linker functionalized metal organic frameworks. *Coord. Chem. Rev.* **2019**, *399*, No. 213023.
- (7) Yin, Z.; Wan, S.; Yang, J.; Kurmoo, M.; Zeng, M. H. Recent advances in post synthetic modification of metal–organic frameworks: New types and tandem reactions. *Coord. Chem. Rev.* **2019**, *378*, 500–512.
- (8) Cohen, S. M. Postsynthetic Methods for the Functionalization of Metal–Organic Frameworks. *Chem. Rev.* **2012**, *112*, 970–1000.
- (9) Deria, P.; Mondloch, J. E.; Karagiari, O.; Bury, W.; Hupp, J. T.; Farha, O. K. Beyond post synthesis modification: evolution of metal–organic frameworks via building block replacement. *Chem. Soc. Rev.* **2014**, *43*, 5896–5912.
- (10) Goto, Y.; Sato, H.; Shinkai, S.; Sada, K. “Clickable” Metal–Organic Framework. *J. Am. Chem. Soc.* **2008**, *130*, 14354–14355.
- (11) Savonnet, M.; Bazer Bachi, D.; Bats, N.; Perez Pellitero, J.; Jeanneau, E.; Lecocq, V.; Pinel, C.; Farrusseng, D. Generic Postfunctionalization Route from Amino Derived Metal–Organic Frameworks. *J. Am. Chem. Soc.* **2010**, *132*, 4518–4519.
- (12) Wang, Z.; Liu, J.; Arslan, H. K.; Grosjean, S.; Hagendorf, T.; Gliemann, H.; Bräse, S.; Wöll, C. Post Synthetic Modification of Metal–Organic Framework Thin Films Using Click Chemistry: The Importance of Strained C–C Triple Bonds. *Langmuir* **2013**, *29*, 15958–15964.
- (13) Kawamichi, T.; Inokuma, Y.; Kawano, M.; Fujita, M. Regioselective Huisgen Cycloaddition within Porous Coordination Networks. *Angew. Chem., Int. Ed.* **2010**, *49*, 2375–2377.
- (14) Liu, C.; Li, T.; Rosi, N. L. Strain Promoted “Click” Modification of a Mesoporous Metal–Organic Framework. *J. Am. Chem. Soc.* **2012**, *134*, 18886–18888.
- (15) von Zons, T.; Brokmann, L.; Lippke, J.; Preuße, T.; Hülsmann, M.; Schaate, A.; Behrens, P.; Godt, A. Postsynthetic Modification of Metal–Organic Frameworks through Nitrile Oxide–Alkyne Cycloaddition. *Inorg. Chem.* **2018**, *57*, 3348–3359.
- (16) Chen, C.; Allen, C. A.; Cohen, S. M. Tandem Postsynthetic Modification of Metal–Organic Frameworks Using an Inverse Electron Demand Diels–Alder Reaction. *Inorg. Chem.* **2011**, *50*, 10534–10536.
- (17) Roy, P.; Schaate, A.; Behrens, P.; Godt, A. Post Synthetic Modification of Zr Metal–Organic Frameworks through Cycloaddition Reactions. *Chem. Eur. J.* **2012**, *18*, 6979–6985.
- (18) Nayab, S.; Trouillet, V.; Gliemann, H.; Hurtle, S.; Weidler, P. G.; Rashid Tariq, S.; Goldmann, A. S.; Barner Kowollik, C.; Yameen, B. Chemically reprogrammable metal organic frameworks (MOFs) based on Diels Alder chemistry. *Chem. Commun.* **2017**, *53*, 11461–11464.
- (19) Gandini, A. The furan/maleimide Diels–Alder reaction: A versatile click–unclick tool in macromolecular synthesis. *Prog. Polym. Sci.* **2013**, *38*, 1–29.
- (20) Goldmann, A. S.; Glassner, M.; Inglis, A. J.; Barner Kowollik, C. Post Functionalization of Polymers via Orthogonal Ligation Chemistry. *Macromol. Rapid Commun.* **2013**, *34*, 810–849.

- (21) Paulöhrli, T.; Inglis, A. J.; Barner Kowollik, C. Reversible Diels Alder Chemistry as a Modular Polymeric Color Switch. *Adv. Mater.* **2010**, *22*, 2788–2791.
- (22) Oehlschlaeger, K. K.; Mueller, J. O.; Brandt, J.; Hilf, S.; Lederer, A.; Wilhelm, M.; Graf, R.; Coote, M. L.; Schmidt, F. G.; Barner Kowollik, C. Adaptable Hetero Diels–Alder Networks for Fast Self Healing under Mild Conditions. *Adv. Mater.* **2014**, *26*, 3561–3566.
- (23) Lowe, A. B. Thiol ene “click” reactions and recent applications in polymer and materials synthesis. *Polym. Chem.* **2010**, *1*, 17–36.
- (24) Hindelang, K.; Kronast, A.; Vagin, S. I.; Rieger, B. Functionalization of Metal–Organic Frameworks through the Postsynthetic Transformation of Olefin Side Groups. *Chem. Commun. Eur. J.* **2013**, *19*, 8244–8252.
- (25) Gui, B.; Hu, G.; Zhou, T.; Wang, C. Pore surface engineering in a zirconium metal–organic framework via thiol ene reaction. *J. Solid State Chem.* **2015**, *223*, 79–83.
- (26) Jiang, W. L.; Ding, L. G.; Yao, B. J.; Wang, J. C.; Chen, G. J.; Li, Y. A.; Ma, J. P.; Ji, J.; Dong, Y.; Dong, Y. B. A MOF membrane based on the covalent bonding driven assembly of a NMOF with an organic oligomer and its application in membrane reactors. *Chem. Commun.* **2016**, *52*, 13564–13567.
- (27) Nair, D. P.; Podgórski, M.; Chatani, S.; Gong, T.; Xi, W.; Fenoli, C. R.; Bowman, C. N. The Thiol Michael Addition Click Reaction: A Powerful and Widely Used Tool in Materials Chemistry. *Chem. Mater.* **2014**, *26*, 724–744.
- (28) Gui, B.; Meng, Y.; Xie, Y.; Tian, J.; Yu, G.; Zeng, W.; Zhang, G.; Gong, S.; Yang, C.; Zhang, D.; Wang, C. Tuning the Photoinduced Electron Transfer in a Zr MOF: Toward Solid State Fluorescent Molecular Switch and Turn On Sensor. *Adv. Mater.* **2018**, *30*, No. 1802329.
- (29) Langer, M.; Brandt, J.; Lederer, A.; Goldmann, A. S.; Schacher, F. H.; Barner Kowollik, C. Amphiphilic block copolymers featuring a reversible hetero Diels Alder linkage. *Polym. Chem.* **2014**, *5*, 5330–5338.
- (30) Schenzel, A. M.; Klein, C.; Rist, K.; Moszner, N.; Barner Kowollik, C. Reversing Adhesion: A Triggered Release Self Reporting Adhesive. *Adv. Sci.* **2016**, *3*, No. 1500361.
- (31) Kerbs, A.; Mueller, P.; Kaupp, M.; Ahmed, I.; Quick, A. S.; Abt, D.; Wegener, M.; Niemeyer, C. M.; Barner Kowollik, C.; Fruk, L. Photo Induced Click Chemistry for DNA Surface Structuring by Direct Laser Writing. *Chem. Eur. J.* **2017**, *23*, 4990–4994.
- (32) Abid, H. R.; Tian, H.; Ang, H. M.; Tade, M. O.; Buckley, C. E.; Wang, S. Nanosize Zr metal organic framework (UiO 66) for hydrogen and carbon dioxide storage. *Chem. Eng. J.* **2012**, *187*, 415–420.
- (33) Dirlam, P. T.; Strange, G. A.; Orlicki, J. A.; Wetzel, E. D.; Costanzo, P. J. Controlling Surface Energy and Wettability with Diels–Alder Chemistry. *Langmuir* **2010**, *26*, 3942–3948.
- (34) Engel, T.; Kickelbick, G. Thermoreversible Reactions on Inorganic Nanoparticle Surfaces: Diels–Alder Reactions on Sterically Crowded Surfaces. *Chem. Mater.* **2013**, *25*, 149–157.
- (35) Patil, D. V.; Rallapalli, P. B. S.; Dangi, G. P.; Tayade, R. J.; Somani, R. S.; Bajaj, H. C. MIL 53(Al): An Efficient Adsorbent for the Removal of Nitrobenzene from Aqueous Solutions. *Ind. Eng. Chem. Res.* **2011**, *50*, 10516–10524.
- (36) Yameen, B.; Alvarez, M.; Azzaroni, O.; Jonas, U.; Knoll, W. Tailoring of Poly(ether ether ketone) Surface Properties via Surface Initiated Atom Transfer Radical Polymerization. *Langmuir* **2009**, *25*, 6214–6220.
- (37) Yameen, B.; Zydziak, N.; Weidner, S. M.; Bruns, M.; Barner Kowollik, C. Conducting Polymer/SWCNTs Modular Hybrid Materials via Diels–Alder Ligation. *Macromolecules* **2013**, *46*, 2606–2615.
- (38) Blinco, J. P.; Trouillet, V.; Bruns, M.; Gerstel, P.; Gliemann, H.; Barner Kowollik, C. Dynamic Covalent Chemistry on Surfaces Employing Highly Reactive Cyclopentadienyl Moieties. *Adv. Mater.* **2011**, *23*, 4435–4439.
- (39) Servalli, M.; Ranocchiari, M.; Van Bokhoven, J. A. Fast and high yield post synthetic modification of metal organic frameworks by vapor diffusion. *Chem. Commun.* **2012**, *48*, 1904–1906.
- (40) Yameen, B.; Rodriguez Emmenegger, C.; Preuss, C. M.; Pop Georgievski, O.; Verveniots, E.; Trouillet, V.; Rezek, B.; Barner Kowollik, C. A facile avenue to conductive polymer brushes via cyclopentadiene maleimide Diels Alder ligation. *Chem. Commun.* **2013**, *49*, 8623–8625.
- (41) Kandiah, M.; Nilsen, M. H.; Usseglio, S.; Jakobsen, S.; Olsbye, U.; Tilset, M.; Larabi, C.; Quadrelli, E. A.; Bonino, F.; Lillerud, K. P. Synthesis and Stability of Tagged UiO 66 Zr MOFs. *Chem. Mater.* **2010**, *22*, 6632–6640.
- (42) Gotthardt, M. A.; Beilmann, A.; Schoch, R.; Engelke, J.; Kleist, W. Post synthetic immobilization of palladium complexes on metal–organic frameworks – a new concept for the design of heterogeneous catalysts for Heck reactions. *RSC Adv.* **2013**, *3*, 10676–10679.
- (43) Faustini, M.; Kim, J.; Jeong, G. Y.; Kim, J. Y.; Moon, H. R.; Ahn, W. S.; Kim, D. P. Microfluidic Approach toward Continuous and Ultrafast Synthesis of Metal–Organic Framework Crystals and Hetero Structures in Confined Microdroplets. *J. Am. Chem. Soc.* **2013**, *135*, 14619–14626.
- (44) Taddei, M.; Tiana, D.; Casati, N.; van Bokhoven, J. A.; Smit, B.; Ranocchiari, M. Mixed linker UiO 66: structure–property relationships revealed by a combination of high resolution powder X ray diffraction and density functional theory calculations. *Phys. Chem. Chem. Phys.* **2017**, *19*, 1551–1559.
- (45) Loiseau, L.; Christian, S.; Clarisse, H.; Gerhard, F.; Francis, T.; Marc, H.; Thierry, B.; Gérard, F. A Rationale for the Large Breathing of the Porous Aluminum Terephthalate (MIL 53) Upon Hydration. *Chem. Eur. J.* **2004**, *10*, 1373–1382.
- (46) Biswas, S.; Ahnfeldt, T.; Stock, N. New Functionalized Flexible Al MIL 53 X (X = Cl, Br, CH<sub>3</sub>, NO<sub>2</sub>, (OH)<sub>2</sub>) Solids: Syntheses, Characterization, Sorption, and Breathing Behavior. *Inorg. Chem.* **2011**, *50*, 9518–9526.
- (47) Hafizovic, J.; Bjørgen, M.; Olsbye, U.; Dietzel, P. D. C.; Bordiga, S.; Prestipino, C.; Lamberti, C.; Lillerud, K. P. The Inconsistency in Adsorption Properties and Powder XRD Data of MOF 5 Is Rationalized by Framework Interpenetration and the Presence of Organic and Inorganic Species in the Nanocavities. *J. Am. Chem. Soc.* **2007**, *129*, 3612–3620.
- (48) Engin, S.; Trouillet, V.; Franz, C. M.; Welle, A.; Bruns, M.; Wedlich, D. Benzylguanine Thiol Self Assembled Monolayers for the Immobilization of SNAP tag Proteins on Microcontact Printed Surface Structures. *Langmuir* **2010**, *26*, 6097–6101.
- (49) Zhang, L.; Vilà, N.; Klein, T.; Kohring, G. W.; Mazurenko, I.; Walcarius, A.; Etienne, M. Immobilization of Cysteine Tagged Proteins on Electrode Surfaces by Thiol–Ene Click Chemistry. *ACS Appl. Mater. Interfaces* **2016**, *8*, 17591–17598.
- (50) Siow, K. S.; Britcher, L.; Kumar, S.; Griesser, H. J. Deposition and XPS and FTIR Analysis of Plasma Polymer Coatings Containing Phosphorus. *Plasma Process. Polym.* **2014**, *11*, 133–141.
- (51) Vahlberg, C.; Linares, M.; Villaume, S.; Norman, P.; Uvdal, K. Noradrenaline and a Thiol Analogue on Gold Surfaces: An Infrared Reflection–Absorption Spectroscopy, X ray Photoelectron Spectroscopy, and Near Edge X ray Absorption Fine Structure Spectroscopy Study. *J. Phys. Chem. C* **2011**, *115*, 165–175.
- (52) Barreca, D.; Gasparotto, A.; Maragno, C.; Tondello, E.; Spalding, T. R. Analysis of Nanocrystalline ZnS Thin Films by XPS. *Surf. Sci. Spectra* **2002**, *9*, 54–61.
- (53) Zhou, Y. Y.; Song, E. H.; Deng, T. T.; Zhang, Q. Y. Waterproof Narrow Band Fluoride Red Phosphor K<sub>2</sub>TiF<sub>6</sub>:Mn<sup>4+</sup> via Facile Superhydrophobic Surface Modification. *ACS Appl. Mater. Interfaces* **2018**, *10*, 880–889.
- (54) Cha, B. J.; Saqlain, S.; Seo, H. O.; Kim, Y. D. Hydrophilic surface modification of TiO<sub>2</sub> to produce a highly sustainable photocatalyst for outdoor air purification. *Appl. Surf. Sci.* **2019**, *479*, 31–38.
- (55) Sun, D.; Xu, M.; Jiang, Y.; Long, J.; Li, Z. Small Sized Bimetallic CuPd Nanoclusters Encapsulated Inside Cavity of NH<sub>2</sub> UiO 66(Zr)

with Superior Performance for Light Induced Suzuki Coupling Reaction. *Small Methods* **2018**, 2, No. 1800164.

(56) Luan, Y.; Qi, Y.; Gao, H.; Andriamitantoa, R. S.; Zheng, N.; Wang, G. A general post synthetic modification approach of amino tagged metal–organic frameworks to access efficient catalysts for the Knoevenagel condensation reaction. *J. Mater. Chem. A* **2015**, 3, 17320–17331.

## Repository KITopen

Dies ist ein Postprint/begutachtetes Manuskript.

Empfohlene Zitierung:

Nayab, S.; Trouillet, V.; Gliemann, H.; Weidler, P. G.; Azeem, I.; Tariq, S. R.; Goldmann, A. S.; Barner-Kowollik, C.; Yameen, B.  
[Reversible Diels-Alder and Michael Addition Reactions Enable the Facile Postsynthetic Modification of Metal-Organic Frameworks](#)  
2021. Inorganic Chemistry  
[10.5445/IR/1000131417](#)

Zitierung der Originalveröffentlichung:

Nayab, S.; Trouillet, V.; Gliemann, H.; Weidler, P. G.; Azeem, I.; Tariq, S. R.; Goldmann, A. S.; Barner-Kowollik, C.; Yameen, B.  
[Reversible Diels-Alder and Michael Addition Reactions Enable the Facile Postsynthetic Modification of Metal-Organic Frameworks](#)  
2021. Inorganic Chemistry, 60 (7), 4397–4409.  
[doi:10.1021/acs.inorgchem.0c02492](#)

Lizenzinformationen: [KITopen-Lizenz](#)